RSC Advances

PAPER

View Article Online
View Journal | View Issue

Cite this: *RSC Adv.*, 2022, **12**, 2009

Hybrid hydrogels derived from renewable resources as a smart stimuli responsive soft material for drug delivery applications†

Vandana Singh,[a] Yadavali Siva Prasad,[ad] Arun Kumar Rachamalla,[c] Vara Prasad Rebaka,[c] Tohira Banoo,[c] C. Uma Maheswari,[a] Vellaisamy Sridharan,[b] Krishnamoorthy Lalitha *[a] and Subbiah Nagarajan *[ac]

Received 18th November 2021
Accepted 29th December 2021

DOI: 10.1039/d1ra08447j

rsc.li/rsc-advances

The design and synthesis of amphiphilic molecules play a crucial role in fabricating smart functional materials *via* self-assembly. Especially, biologically significant natural molecules and their structural analogues have inspired chemists and made a major contribution to the development of advanced smart materials. In this report, a series of amphiphilic *N*-acyl amides were synthesized from natural precursors using a simple synthetic protocol. Interestingly, the self-assembly of amphiphiles **6a** and **7a** furnished a hydrogel and oleogel in vegetable oils. Morphological analysis of gels revealed the existence of a 3-dimensional fibrous network. Thermoresponsive and thixotropic behavior of these gels were evaluated using rheological analysis. A composite gel prepared by the encapsulation of curcumin in the hydrogel formed from **7a** displayed a gel–sol transition in response to pH and could act as a dual channel responsive drug carrier.

Introduction

Self-assembly is a natural process accomplishing a key role in the origin, maintenance, and growth of life.[1–5] Inspired by natural phenomena, the interest in the assembly of bio-macromolecules and low molecular weight gelators (LMWGs) to fabricate biomimetics, and functional materials for practical applications has increased significantly.[1–5] Gels are a kind of smart material possessing a 3D supramolecular network displaying visco-elastic behaviour *via* the self-organization of amphiphiles in a suitable solvent involving reversible non-covalent interactions such as van der Waals forces, hydrogen bonding, metal–ligand coordination, anionic-π, cationic-π, and CH–π interactions, and π–π stacking.[3] In assembled materials, a finite tuning in molecular level interaction is observed upon the exposure to external stimuli, which enable them to behave as a prospective soft material suitable for a wide range of applications such as wound healing, bone-repair, drug delivery, sensors, imaging, to name a few.[1–5] Owing to the potential applications of these soft materials, we are interested in the design and synthesis of the amphiphiles with an amide bond from the natural molecules, that could display molecular self-assembly. It is worth mentioning that, an effective balance of hydrophilicity and lipophilicity (HLB) is essential for construction of 3-D supramolecular architecture.[6,7] Generally, amphiphiles derived from amino alcohols, amino acids, hydrazides, carbohydrates, peptides, to name a few, display various degree of HLB to furnish different supramolecular architecture. Among these building blocks, amino alcohols are of much industrial importance on account of their potential usefulness in the manufacture of pharmaceuticals, surfactants, agrochemicals and lubricating oil additives.[8] In the past 2 decades, gelators derived by molecular self-assembly of amino alcohol such as bis(amino acid)oxalamides,[9] bis(amino alcohol)oxalamides,[9,10] bis(aminoalcohol)diglycolamides,[10] bis(phenylglycinol)malonamide,[11] lipopeptides were extensively studied and their potential application in biology and medicine were explored.[12,13] It is worth mentioning that dopamine an important amino alcohol largely explored in the field of medicine, coatings, water purification, sensors energy storage, and disease treatment.[14–25] However, there is not much research on the use of dopamine for the generation of amphiphilic molecules. By looking at the broad applications of soft materials derived from biomolecules and renewable resources, in this paper, we have selected amino alcohols like propanol amine, tris and dopamine as a moiety rendering hydrophilicity, and cardanol, an alkyl phenolic oil extracted from the cashew nutshell, as one of the renewable

[a]*School of Chemical and Biotechnology, SASTRA Deemed University, Thanjavur-613401, Tamil Nadu, India. E-mail: lalitha@scbt.sastra.edu*

[b]*Department of Chemistry and Chemical Sciences, Central University of Jammu, Rahya-Suchani (Bagla), District-Samba, Jammu-181143, J&K, India*

[c]*Department of Chemistry, National Institute of Technology Warangal, Warangal-506004, Telangana, India. E-mail: snagarajan@nitw.ac.in; Tel: +91-9940430715*

[d]*Department of Biomedical Engineering, Saveetha School of Engineering, Saveetha Nagar, Thandalam, Tamil Nadu, India*

† Electronic supplementary information (ESI) available. See DOI: 10.1039/d1ra08447j

value-added raw materials for the synthesis of amphiphilic *N*-acyl amide derivatives.

Cardanol is a bio-based phenolic lipid mixture comprising 50% of 3-(8*Z*-pentadecenyl)phenol, 16% of 3-(8*Z*,11*Z*-pentadecadienyl)phenol, 29% of 3-(8*Z*,11*Z*,14-pentadecatrienyl)phenol and 5% of 3-(*n*-pentadecyl)phenol.[26–30] The presence of a phenolic moiety and the long alkyl chain with varying degrees of unsaturation at *meta*-position provides the unique characteristics to cardanol and enables the self-assembly *via* π–π stacking and hydrophobic interactions.[26–30] In this line, John and co-workers reported the synthesis of phenoxyacylethanolamides from this CNSL and studied their amidohydrolase activity of fatty acid amide hydrolase (FAAH).[31] In this paper, we report a facile synthesis of amphiphilic *N*-acyl amides by the judicious combination of various amino alcohols such as dopamine, propanol amine, and tris, and the phenolic esters derived from cardanol and explored their molecular self-assembly in a wide variety of solvents and vegetable oils. We have also demonstrated the potential application of one of the amphiphilic *N*-acyl amides as a dual channel stimuli-responsive delivery system for the natural hydrophobic drug, curcumin. Further, supramolecular architecture and stimuli responsive behaviour were investigated with respect to the molecular structure.

Results and discussion

Inspired by the natural self-assembly of proteins, amino acids, nucleic acids, and lipids in biological systems, the interest in the design and synthesis of amphiphiles to fabricate functional soft materials by exploiting their molecular self-assembly has raised significantly. Recently, we have reported the synthesis and self-assembly of cardanol-based functional molecules and explored their potential applications in the field of biomaterials and electronics.[32–37] The excellent antioxidant property and self-assembling characteristics of largely explored fatty acid amides elicited us to design and synthesize the amphiphilic *N*-acyl amides from cardanol and amino alcohols such as propanol amine **4**, tris **5**, and dopamine **8**. Amphiphilic *N*-acyl amides (**6**, **7**) bearing aliphatic OH group as a hydrophilic moiety were synthesized *via* the nucleophilic substitution of 3-alkyl phenols **1a,b** with methyl bromoacetate **2**, followed by amidation with amino alcohols **4**, and **5** (Scheme 1).[31,37] Amphiphilic *N*-(3-hydroxypropyl)-2-(3-alkyl phenoxy)acetamides **6a,b** bearing an aliphatic OH group was prepared by following the procedure reported in the literature.[31]

The formation of the desired product was confirmed using NMR and mass spectral analysis. In ^{1}H NMR spectrum of compound **6a**, the peak at δ 6.94 and 4.51 ppm represent –NH and –OCH_2– protons, and in ^{13}C NMR spectra, the peak at δ 169.6 and 67.1 ppm represent the carbonyl and –OCH_2– group respectively. A separate reaction condition suitable for the synthesis of amphiphilic *N*-(1,3-dihydroxy-2-(hydroxymethyl) propan-2-yl)-2-(3-alkyl phenoxy)acetamides, **7a,b** bearing three aliphatic OH groups was optimized using solvents such as MeOH, EtOH, DCM, DMSO, and THF by varying the temperature and reaction time (Table S1†). Amphiphilic *N*-acyl amides

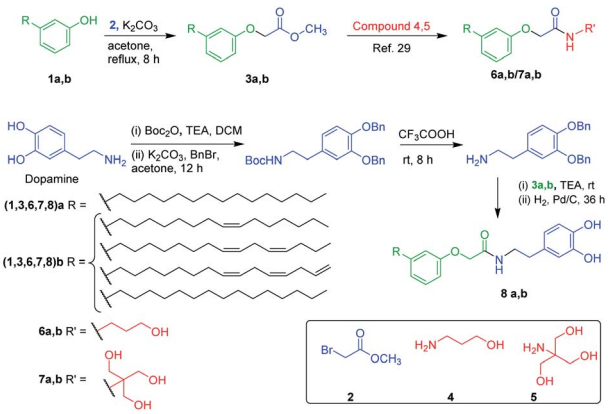

Scheme 1 Synthesis of *N*-acyl amides-based amphiphiles (6–8)a,b.

(**8a,b**) bearing aromatic OH moiety were synthesized by following Scheme 1. Direct amidation of dopamine with **3a,b** resulted in the polymerization of dopamine.[25] In order to avoid the polymerization during the synthesis of compounds **8a,b** we have adopted the protected/deprotection strategy as given in Scheme 1. The formation of compounds **8a,b** was identified using NMR and mass spectral analysis (Fig. S17–S25, ESI†).

By having amphiphilic *N*-acyl amides bearing various degree of hydrophilic groups, we further moved on investigating the gelation efficiency in various solvents and vegetable oils using the "stable to inversion" method.[32–40] Most interestingly,

Table 1 Gelation studies of compounds (6–8)a,b in various solvents and vegetable oils

		Observation[a]					
S. No.	Solvent/oil	**6a**	**6b**	**7a**	**7b**	**8a**	**8b**
1	Olive oil	S	S	S	S	S	S
2	Heavy paraffin oil	S	S	S	S	S	S
3	Light paraffin oil	G (1.0%)	S	G (0.9%)	S	S	S
4	Sesame oil	S	S	S	S	S	S
5	Linseed oil	S	S	S	S	S	S
6	Water	I	I	I	I	I	S
7	Water + DMSO (3 : 1)	G (1.3%)	S	G (1.0%)	S	S	S
8	DMF	S	S	S	S	S	S
9	Ethyl acetate	I	S	I	S	S	S
10	Cyclohexane	S	S	S	S	S	S
11	Jojoba oil	S	S	S	S	S	S
12	Castor oil	S	S	S	S	S	S
13	Xylene	S	S	S	S	S	S
14	Glycerol	S	S	S	S	S	S
15	Ethylene glycol	S	S	S	S	S	S
16	Soya bean oil	S	S	S	S	S	S
17	Eucalyptus oil	S	S	S	S	S	S
18	Buffer	I	I	I	I	S	S
19	Hazel nut oil	S	S	S	S	S	S
20	Poly ethylene glycol	G (1.0%)	S	G (0.85%)	S	S	S
21	Methanol	S	S	S	S	S	S
22	1,2-Dichlorobenzene	S	S	S	S	S	S
23	Lauryl alcohol	S	S	S	S	S	S

[a] Critical gelation concentration is given in % w/v within parenthesis, S – soluble; I – insoluble; G – gelation.

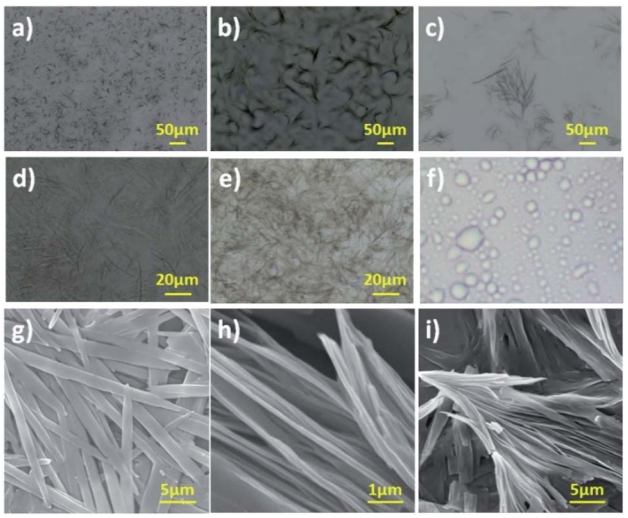

Fig. 1 (a–f) Optical micrograph of gel formed by (a and b) **6a** in DMSO + H_2O (1 : 3), (c) **6a** in poly(ethylene glycol), (d) **6a** in light paraffin, (e) **7a** in DMSO + H_2O (1 : 3). (f) Micellar structure formed by **8a** in DMSO–water (1 : 3). (g–i) SEM images of the gel formed by (g) **6a** and (h and i) **7a** in DMSO + H_2O (1 : 3) respectively. Gel formed in DMSO + H_2O (1 : 3) is referred as hydrogel.

compounds **6a** and **7a** displayed oleogelation in light paraffin oil with the critical gelation concentration (CGC) of 1.0 and 0.9% (w/v) respectively. In addition, compounds **6a** and **7a** also formed organogel in PEG with a CGC of 1.0 and 0.85% (w/v), and hybrid hydrogel in water–DMSO (3 : 1) with a CGC of 1.3% (w/v) and 1.0% (w/v) respectively (Table 1). The existence of a kink in the hydrophobic part of the amphiphilic *N*-acyl amides **6b** and **7b** belittled their gelation behaviour with respect to the corresponding saturated moieties. *N*-Acyl amides, **8a** and **8b** bearing aromatic OH as hydrophilic part did not show any gelation in the tested solvent and vegetable oil, instead formed micelles in an ethanol–water mixture (1 : 9) (Fig. 2a(iv)). It is worth mentioning that, compounds **8a** and **8b** bearing aromatic OH (pK_a: ~9) did not form gel even at basic pH levels, for the reason that the phenolic OH can dissociate into ionic form, there by tune the hydrophilicity. Overall, to our surprise, *N*-acyl amides bearing aliphatic OH group as hydrophilic part displayed gelation in both highly hydrophobic solvent (paraffin oil) and hydrophilic solvent (polyethylene glycol and water), whereas compound bearing aromatic OH group as hydrophilic part did not show molecular self-assembly to form a gel. In order to identify the thermal stability of gels, we have determined gel-to-sol transition temperature (T_{gel}) of the gels formed by **6a** and **7a**.[39,41] T_{gel} of **6a** in light paraffin oil, PEG and DMSO:water mixture was observed as 84, 87 and 75 °C respectively. Surprisingly, compound **7a**, which is having more hydroxyl group displayed increased T_{gel} in light paraffin oil, PEG and DMSO:water system such as 82, 89 and 85 °C respectively. The presence of more hydroxyl groups in compound **7a** might enhance the intensity of H-bonding in DMSO:water system, thereby increasing the gel-to-sol transition temperature.

Morphological analysis

Generally, aggregation of a gelator to generate supramolecular architecture in micro or nanoscale is based on the molecular structure of the gelator, solvent used, temperature and pressure.[32–42] However, properties of soft materials were governed by the molecular assembly, which requires a clear understanding across length scales controlled by intermolecular interactions. In order to probe gel morphology and gelation mechanism, microscopic analysis of xerogel formed by amphiphilic *N*-acyl amides **6a** and **7a** was performed using optical microscopy, and

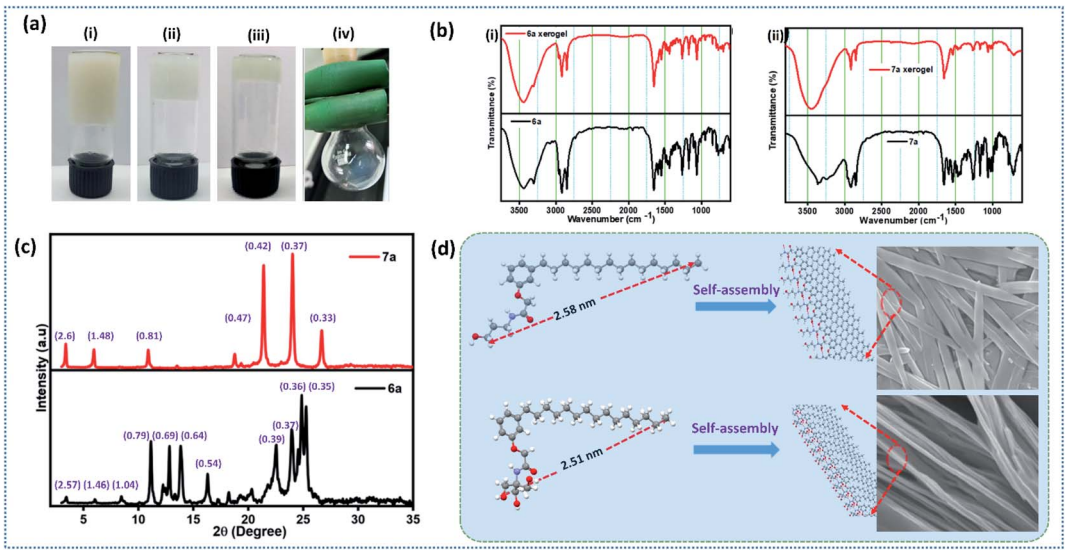

Fig. 2 a) Gel images of (i) **6a** in light paraffin oil, (ii) hydrogel derived from **6a**, (iii) hydrogel derived from **7a** (iv) **8a** in DMSO–water (1 : 3); (b) ATR-IR spectra of the compound (i) **6a** and (ii) **7a** in amorphous and xerogel respectively; (c) SAXRD of xerogel formed by **6a** and **7a**; (d) pictorial representation of molecular self-assembly of compound **6a** (top) and **7a** (bottom) respectively. Intermolecular H-bonding is represented in red dotted line.

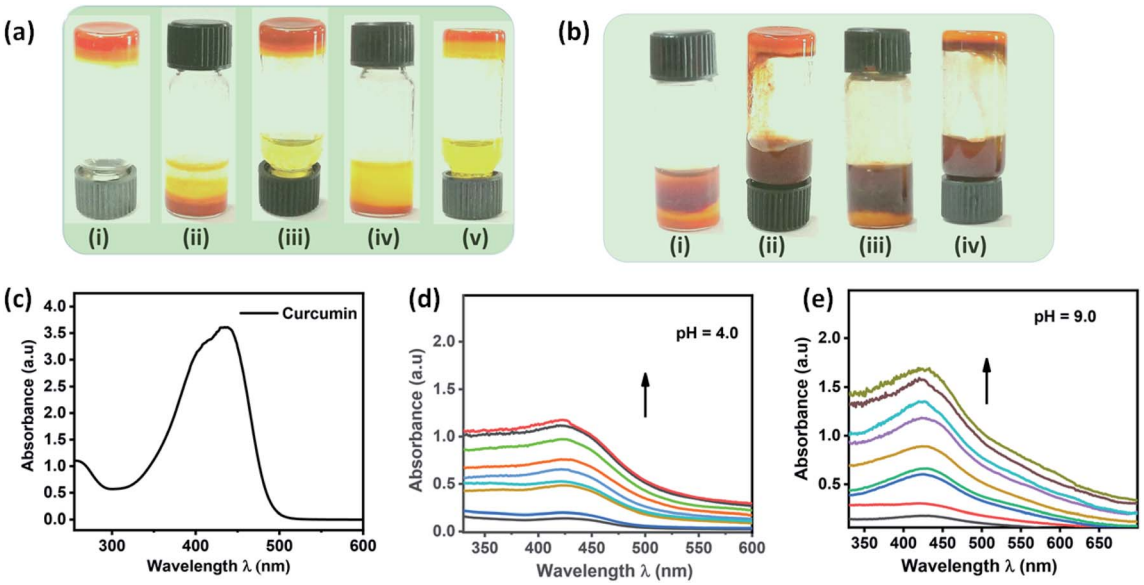

Fig. 3 (a) Images of (i) curcumin encapsulated gel formed by compound **7a**, (ii–v) addition of buffer of pH 4.0 and inverted vial displaying the natural drug, curcumin release with respect to time respectively, (b) images of (i) addition of buffer of pH = 9.0 (ii–iv) pH responsive curcumin release after 10 and 30 minutes respectively, (c) UV-vis spectrum of curcumin dissolved in MeOH, (d and e) curcumin release profile of gel formed by **7a** under the influence of acidic and basic buffer.

scanning electron microscopy (SEM).[42] Optical microscopy images of gel formed by **6a** and **7a** were given in Fig. 1a–e. Gel formed by **6a** in DMSO–water (1 : 3), polyethylene glycol and light paraffin oil display a micro or nanoscale fibrillar structure generating a 3D entangled network (Fig. 1a–d). Assembly pattern of compound **7a** in DMSO–water (1 : 3) furnishes bundled fibers with entanglement, whereas **8a** in DMSO–water (1 : 3) did not form gel instead display a micelle like morphology (Fig. 1e and f). The average size of the micelles were analysed using a particle size analyser, which displayed an average size of 400 nm (Fig. S27†).

Optical microscopic analysis clearly revealed the existence of distinct morphology, which is based on the molecular structure and solvent used. Further, we have performed SEM analysis to get a clear cut morphology of hydrogel formed by **6a** and **7a** (Fig. 1g–i and S26†). Hydrogel obtained from compound **6a** displayed lamellar morphology of width ranging from 1.0–1.5 μm, whereas compound **7a** rendered a bundled fibrillar

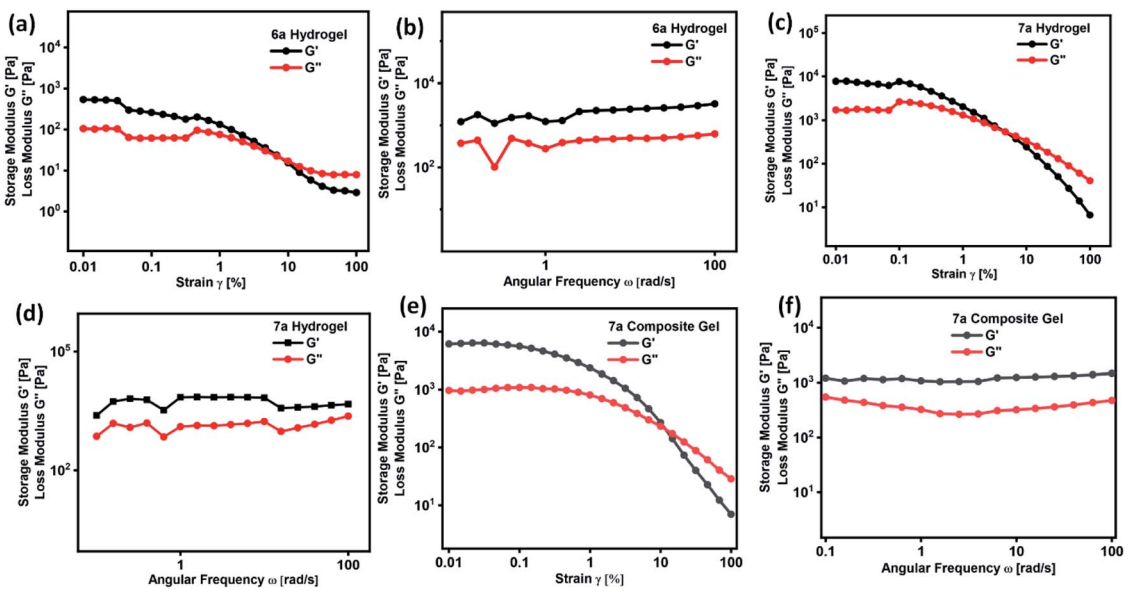

Fig. 4 Strain amplitude and angular frequency dependence of storage (G') and loss modulus (G'') of hydrogel formed by (a and b) **6a**, (c and d) **7a** and (e and f) composite hydrogel of **7a** respectively.

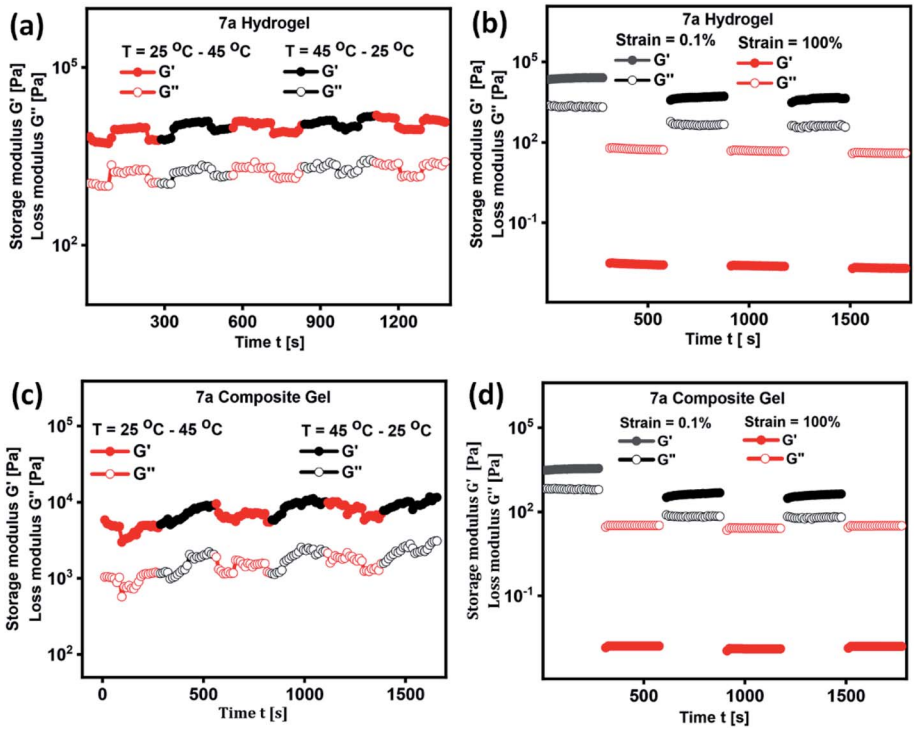

Fig. 5 Temperature dependence and time course change of G' and G'' in the continuous step-strain measurements of (a and b) hydrogel of **7a** and (c and d) composite hydrogel of **7a** respectively.

architecture of width ranging from 500–800 nm (Fig. 1g–i). It is worth discussing that the small tuning in the hydrophilicity of *N*-acyl amides drastically change the self-assembly behaviour and morphology. The replacement of aliphatic OH in compound **6** and **7** with aromatic OH (**8a,b**) resulted in the formation of micelles (Fig. S27†). In addition to the molecular tuning, change in solvent also influence the aggregation pattern of amphiphilic *N*-acyl amides (Fig. 1).[43,44]

Interesting results obtained on the gelation and morphology further inspired us to look into the detailed packing pattern of gelator using intermolecular interactions. ATR-IR spectroscopic analysis of compounds **6a** and **7a** in amorphous and self-assembled form (xerogel) is given in Fig. 2b. Compound **6a** in amorphous state displayed absorption band at ν = 3443 (–OH, H-bonded), 3305 (–NH), 2955 (–CH, alkane), 2917 (–CH, alkane), 2847 (–CH, alkane), 1648 (–C=O, amide), 1589 (–C=C bending, aromatic), and 1550 (–NH bending) cm^{-1}, whereas in xerogel state showed absorption band at ν = 3451 (–OH, H-bonded), 3302 (–NH), 2969 (–CH, alkane), 2916 (–CH, alkane), 2847 (–CH, alkane), 1648 (–C=O, amide), 1592 (–C=C bending, aromatic), and 1551 (–NH bending) cm^{-1}. Analysis of IR data revealed that the existence of random molecular aggregation in amorphous state facilitated by intermolecular H-bonding, whereas in xerogel state, in addition to intermolecular H-bonding, π–π stacking and hydrophobic interactions in long alkyl chain are clearly visualized (Fig. 2b).[45,46] Compound **7a** displayed IR absorption band at ν = 3365, 3340, 3239, 2960, 2920, 2846, 1662, 1591 and 1540 cm^{-1} in amorphous form, and 3450, 2917, 2846, 1654, 1628, 1535 cm^{-1} in the xerogel state. The appreciable shift in bands corresponding to –OH, –NH, –CH (alkane), –C=C (Ar), –CH (Ar), –C=O (amide) clearly reveal the establishment of strong intermolecular interaction during the self-assembly process.[46] IR data analysis of **6a** and **7a** in amorphous and xerogel state reveal that compound **7a** upon self-assembly establish a strong intermolecular interactions than **6a**, which could be clearly visualized from the significant shift in absorption frequency (cm^{-1}).

Small angle X-ray diffraction (SAXRD) studies

To explore the dynamic gelation due to molecular packing, low angle powder XRD was used. SAXRD pattern of the xerogel obtained from compound **6a** and **7a** is given in Fig. 2c. Xerogel of the **6a** displayed Bragg's reflection at 2θ = 3.44°, 6.05°, 8.46°, 11.14°, 12.82°, 13.85°, 16.31°, 22.54°, 23.97°, 24.86°, 25.26° corresponding to the *d*-spacing of 2.57, 1.46, 1.04, 0.79, 0.69, 0.64, 0.54, 0.39, 0.37, 0.36, 0.35 nm (Fig. 2c), whereas **7a** displayed a well distinct peaks at 2θ = 3.40°, 5.96°, 10.90°, 18.77°, 21.40°, 24.03°, 26.69°, with *d*-spacing of 2.6, 1.48, 0.81, 0.47, 0.42, 0.37, 0.33 nm respectively. It is worth mentioning that peaks of **6a** and **7a** are not at the same position indicating the different packing pattern. However, peaks of **7a** is well resolved and distinct in nature when compared to **6a**. In order to establish the packing arrangement involving various inter and intermolecular interactions, energy minimized structure were obtained and their molecular length were calculated and compared with experimental XRD diffraction data. XRD of compound **6a** and **7a** furnished *d*-spacing value of 2.57 and 2.6 nm, which is almost equal to their corresponding molecular

length of 2.58 and 2.51 nm respectively. The observed *d*-spacing value clearly reveals the existence of monolayer arrangement forming the fibrillar structure.[47] Further, small tuning in the hydrophilic part of an amphiphile display different packing arrangement in molecular level generating drastic change in morphological structure in gels.

Spectral and morphological studies clearly revealed that the tuning of intermolecular interaction, especially H-bonding in the hydrophilic part can change the self-assembly. pK_a value of primary alcohol is around 16.0 and generally considered as weak Brønsted acid and base.[48] However, the dissociation of alcohol can be achieved by tuning the pH of the medium.[48] Since the system selected for our investigation is having amide linkage and varying degree of hydroxyl group, we were curious to check the pH responsive behaviour of self-assembled monolayer fibrils formed from **6a** and **7a** under varying pH. Acidic buffer of pH 4.0 and basic buffer of pH 9.0 was added slowly over the hydrogel and observed their influence. Interestingly, a rapid gel to sol was observed in basic buffer, whereas a slow and steady trend of gel to sol transition was observed in an acidic buffer (Fig. 3a and b), which clearly reveals the disassembly of fibrils formed by monolayer arrangement.[49] Percolation of acidic and basic buffer into the gel further tune the intermolecular H-bonding interaction, facilitating gel-to-sol transition, which could be visualized by the naked eye (Fig. 3a and b). It is worth mentioning that the gel formed by **6a** and **7a** were highly stable in neutral pH for a long period. Molecular packing and pH responsive behaviour of hydrogel prompted us to investigate the practical utility of these gels in stimuli responsive delivery of the natural hydrophobic drug, curcumin. While forming hydrogel, we have encapsulated a hydrophobic drug, curcumin in the ratio of 2 : 1 and subsequently studied the drug release profile under acidic and basic pH. On to the curcumin encapsulated composite hydrogel formed from compound **7a** in the ratio of 2 : 1 (ratio of gelator to curcumin load), we have added 15 mL of buffer solution and monitored their release profile using UV-vis spectrometer by withdrawing 1 mL supernatant solution at 10 minutes intervals. Fig. 3c–e reveals the absorbance of curcumin and drug release profile of gel under the influence of acidic and basic buffer respectively. Aliquot collected at 5 minutes time intervals displayed the absorbance of curcumin and an increase in absorption intensity with respect to time was also observed. It should be noted that acidic buffer as an external stimulus released yellow solution from the encapsulated gel, whereas the use of basic buffer generated light brown solution. However, there is no drastic change in λ_{max} of released curcumin. Stimuli-responsive release of the encapsulated drug by acidic and basic buffer could be attributed to H-bonding triggered assembly and disassembly of monolayer fibres, which address the problems associated with the solubilisation of hydrophobic drugs and formulation of dual channel stimuli responsive delivery systems.

Rheological analysis

A defined extent of material deformation from its original state in response to a force applied is generally narrated by rheological measurements. In particular, a deep insight into a flow and viscoelastic behaviour of a soft material, which belongs to a unique category neither behave like ideal solid and nor ideal liquid were obtained by measuring the storage modulus G' (elastic) and the loss modulus G'' (viscous) in response to the strain.[32–37,50,51] Such an interesting deformation of a soft material in response to stress or strain is due to the internal morphology drew up with the supra-molecular arrangement of small or macromolecules and colloidal organic/inorganic particles. However, till to date there is no direct correlation were derived between the internal morphology and viscoelastic behaviour of soft materials, in particular, many of the questions related to the micro/nanostructure and viscoelastic behaviour remain unanswered. In order to realize the practical utility of these gels in medicine or drug formulation, a clear cut understanding of soft material rheology is needed. Rheological measurement of hydrogel formed by compound **6a** and **7a** is given in Fig. 4. Initially, the response of G' and G'' with respect to strain sweep and frequency sweep was investigated in detail. Strain amplitude sweep measurements revealed that within the range of linear viscoelastic region (LVE), $G' > G''$ suggesting the existence of gel like structure with good mechanical strength (Fig. 4a and c). Interestingly, in the entire range of frequency sweep test, the storage modulus G' is greater than loss modulus G'' clearly reveal the stability and good tolerance towards the external forces of the hydrogels formed by **6a** and **7a** (Fig. 4b and d). It is worth mentioning that the surface of the soft material derived from **6a** and **7a** form a slight depression or fold in its smoothness beyond the critical strain (γ_c) value of 0.83 and 0.35% and complete gel to sol transformation was observe at $\gamma = 7.92\%$, and 4.8% respectively (Fig. 4a and c). Curcumin encapsulated composite hydrogel prepared from compound **7a** displayed good stability, and no physical change were observed even after 120 days. When compared to hydrogel of **7a**, composite hydrogel displayed an increase in critical strain (γ_c) value of from 0.35 to 1.5% and gel to sol transition strain from 4.8% to 12.1%, which clearly reveal the uniform intercalation of hydrophobic drug curcumin in the self-assembled fibrillar monolayer structure, thereby enhancing the mechanical behaviour (Fig. 4e). Nevertheless the storage modulus G' of the hydrogel and composite gel of compound **7a** is greater than **6a** indicating the enhanced stiffness.

In the development of materials science and technology, plenty of assembled systems derived from polymers, small molecules and inorganic nanoparticles were studied for their delivery of biotherapeutics. However, thermo-reversible hydrogels derived from renewable raw materials have received great attention because of their resemblance with living tissues and biocompatibility.[52] In order to validate the thermal processability of hydrogel in the field of drug formulation, bioengineering and drug delivery, we have performed continuous temperature ramp-up and ramp-down experiments. Hydrogel and composite gel derived from **7a** displayed good thermal stability and processability even after several temperature ramp up and down cycles (Fig. 5a and c). Thixotropic behaviour of hydrogels were studied by a continuous step-strain experiment

(Fig. 5b and d). Upon the application of high strain (100%), storage modulus G' is found to be lower than the loss modulus G'' indicating the development of folds followed by the destruction of 3D-network in hydrogel. Once the strain is reduced to 1%, a higher G' value is observed, which clearly reveal the rapid recovery of gel to its original structure by the reconstruction of fibrillar network (Fig. 5b and d). Thixotropic behaviour of hydrogels and composite gel were consistent even after 4 cycles of step-strain experiment.

Conclusion

In summary, a set of three structurally similar amphiphilic-*N*-acyl amides were synthesized from renewable raw materials and biologically significant natural substrates and well characterized by NMR and mass spectral techniques. A simple protocol was adopted to synthesize amphiphilic *N*-acyl amides and the self-assembly of two interesting amphiphiles **6a** and **7a** furnished hydrogel and oleogel in vegetable oils. Morphological analysis of gels revealed the existence of lamellar and bundled fibrillar architecture. Interestingly, a fine tuning of hydrophilicity in *N*-acyl amides drastically change the self-assembly behaviour and morphology, which clearly reveal the existence of different degree of intermolecular interactions. Self-assembly mechanism has been proposed based on gelation studies, XRD and FT-IR techniques. Rheological studies clearly revealed the details related to the deformation of gel with respect to stress or strain, which is solely depend on the internal morphology drew up with the supra-molecular arrangement of gelators. The existence of thermoresponsive and thixotropic behaviour of these gels were established by rheological studies. Interesting hydrogel formed from **7a** exhibited gel to sol transition in response to pH. In order to realize the practical application of hydrogel formed from **7a**, a composite gel was prepared by the encapsulation of curcumin and gel–sol transition in response to pH were studied in detail. We envision that this dual channel responsive drug carrier could play a significant role in medical and pharmaceutical sciences, in particular for the development of advanced stimuli responsive drug delivery systems.

Experimental section

Materials and general methods

All the essential reagents and solvents needed for the synthesis of *N*-acyl amides-based amphiphiles were purchased from Alfa Aesar, Sigma Aldrich, Merck, Avra chemicals, Loba, SRL and used as such without any further purification. LR grade solvents and distilled solvents were used when necessary. Thin-layer chromatography using pre-coated silica gel plates purchased from Merck was employed to monitor the reaction progress and visualized by UV detection or *p*-anisaldehyde stain or molecular iodine. Column chromatography was performed with silica gel (60–120 mesh) purchased from Avra chemicals. ^{1}H- and ^{13}C-NMR spectra for amphiphilic *N*-acyl amides and their precursors were recorded on a Bruker Avance 300 MHz instrument in $CDCl_3$ at room temperature. Chemical shifts (δ) are reported in parts per million (ppm) using TMS as internal standard and coupling constants (J) are given in Hz. Proton multiplicity is assigned using the following abbreviations: singlet (s), doublet (d), triplet (t), quartet (q), and multiplet (m). Electrospray ionization mass spectra (ESI-MS) were carried out in positive mode with a Thermo Fisher LCQ Advantage Max. instrument by dissolving the solid sample in methanol.

Synthesis

General procedure for the synthesis of methyl 2-(3-alkyl phenoxy)acetates (3a and 3b). To the stirred solution of 3-alkyl phenols **1a** and **1b** (2.0 mmol) in acetone (5.0 mL), added methyl bromoacetate **2** (2.0 mmol), anhydrous K_2CO_3 (4.0 mmol), and refluxed for 8 h. The reaction progress was monitored using TLC. After identifying the completion of the reaction using TLC, the reaction mixture was cooled to room temperature and added water to dissolve the solid residues. The crude product extracted with ethyl acetate was purified by employing the silica gel column (100–200 mesh) using a 2% ethyl acetate–hexane mixture. Methyl esters **3a** and **3b** were obtained in good yields (**3a**: 95% and **3b**: 92%).[31,37]

General procedure for the synthesis of *N*-(3-hydroxypropyl)-2-(-3-alkyl phenoxy)acetamides 6a,b. To the stirred solution of methyl 2-(3-alkyl phenoxy)acetates **3a,b** (1.0 mmol) in dichloromethane (3 mL) and triethylamine (1.2 mmol), added propanol amine **4** in drops under nitrogen atmosphere in an ice bath with constant stirring for 30 minutes. The resultant reaction mixture was further stirred at room temperature for about 8 h. The progress of the reaction was monitored using TLC. After the completion of the reaction, as identified by TLC, the product is extracted with dichloromethane and purified using column chromatography.[18]

*Compound **6a**.* Isolated as white solid; melting point = 48–50 °C; yield = 82%; ^{1}H NMR (300 MHz, $CDCl_3$) δ = 7.22 (t, J = 7.8 Hz, 1H, Ar–*H*), 6.94 (s (br), 1H, –N*H*), 6.86 (d, J = 7.8 Hz, 1H, Ar–*H*), 6.75–6.70 (m, 2H, Ar–*H*), 4.51 (s, 2H, –O–C*H*$_2$–), 3.65 (t, J = 5.6 Hz, 2H, –C*H*$_2$–), 3.53 (q, J = 6.3 Hz, 2H, –C*H*$_2$), 2.58 (t, J = 7.7 Hz, 2H, –C*H*$_2$), 1.77–1.70 (m, 2H, –C*H*$_2$), 1.62–1.54 (m, 2H, –C*H*$_2$), 1.29–1.24 (m, 24H, –C*H*$_2$), 0.88 (t, J = 6.9 Hz, 3H, –C*H*$_3$); ^{13}C NMR (75 MHz, $CDCl_3$) δ = 169.6, 157.1, 145.1, 129.4, 122.3, 114.8, 111.6, 67.1, 59.3, 35.9, 35.8, 32.1, 31.9, 31.3, 29.7, 29.6, 29.6, 29.5, 29.3, 29.3, 22.6, 14.1; HRMS(ESI) m/z calculated for $C_{26}H_{45}NO_3$ = 420.3477 $[M + H]^+$; observed = 420.3482.

*Compound **6b**.* Isolated as yellow semi-solid; yield = 78%; ^{1}H NMR (300 MHz, $CDCl_3$) δ = 7.22 (t, J = 7.7 Hz, 1H, Ar–*H*), 6.95 (s (br), 1H, –N*H*), 6.86 (d, J = 7.5 Hz, 1H, Ar–*H*), 6.74–6.70 (m, 2H, Ar–*H*), 5.39–5.33 (m, 2H, –C*H*=C*H*), 4.52 (s, 2H, –O–C*H*$_2$), 3.65 (t, J = 5.7 Hz, 2H, –C*H*$_2$), 3.53 (q, J = 6.3 Hz, 2H, –C*H*$_2$), 2.58 (t, J = 7.8 Hz, 2H, –C*H*$_2$–Ar), 2.09–1.96 (m, 2H, –C*H*$_2$), 1.78–1.69 (m, 4H, –C*H*$_2$), 1.65–1.57 (m, 4H, –C*H*$_2$), 1.30–1.22 (m, 14H, –C*H*$_2$), 0.88 (t, J = 6.6 Hz, 3H, –C*H*$_3$); ^{13}C NMR (75 MHz, $CDCl_3$) δ = 169.5, 157.1, 145.0, 129.9, 129.7, 129.4, 122.3, 114.8, 111.6, 67.1, 59.3, 36.0, 35.9, 32.5, 32.0, 31.8, 31.7, 31.6, 31.3, 29.6, 29.5, 29.3, 29.1, 28.9, 27.2, 27.1, 22.6, 14.1.

General procedure for the synthesis of *N*-(1,3-dihydroxy-2-(hydroxymethyl)propan-2-yl)-2-(3-alkyl phenoxy)acetamides 7a,b. To the stirred solution of methyl 2-(3-alkyl phenoxy)

acetates **3a** and **3b** (1.0 mmol) in dichloromethane (3 mL) and triethylamine (1.2 mmol), added the solution of tris **5** (1.0 mmol) dissolved in methanol in drops under nitrogen atmosphere with constant stirring for about 12 h. The progress of the reaction was monitored using TLC. After the completion of the reaction, as identified by TLC, the product is extracted with dichloromethane and recrystallized in methanol.

*Compound **7a**.* Isolated as white solid; melting point = 85–87 °C; yield = 72%; ^{1}H NMR (300 MHz, $CDCl_3$) δ = 7.69 (s, 1H, –N*H*–), 7.21 (t, J = 7.8 Hz, 1H, Ar–*H*), 6.86 (d, J = 7.8 Hz, 1H, Ar–*H*), 6.76–6.72 (m, 2H, Ar–*H*), 4.51 (s, 2H, –O–CH_2CO), 3.99 (s, 3H, –O*H*), 3.69 (s, 6H, –CH_2OH), 2.57 (t, J = 7.8 Hz, 2H, –CH_2–Ar), 1.61–1.54 (m, 2H, –CH_2), 1.30–1.06 (m, 24H, –CH_2), 0.0.88 (t, J = 6.5 Hz, 3H, –CH_3); ^{13}C NMR (75 MHz, $CDCl_3$) δ = 168.7, 155.6, 143.9, 128.2, 121.2, 113.8, 110.4, 66.0, 64.0, 61.0, 60.4, 51.0, 34.7, 30.6, 30.1, 30.0, 28.4, 28.4, 28.3, 28.2, 28.1, 28.0, 21.4, 12.8. HRMS (ESI) m/z calculated for $C_{27}H_{47}NO_5$ = 466.3532 $[M + H]^+$; observed = 466.3557.

*Compound **7b**.* Isolated as yellow viscous liquid; yield = 70%; ^{1}H NMR (300 MHz, $CDCl_3$) δ = 7.69 (s, 1H, –N*H*), 7.22 (t, J = 7.5 Hz, 1H, Ar–*H*), 6.86 (d, J = 8.1 Hz, 1H, Ar–*H*), 6.78–6.72 (m, 2H, Ar–H), 5.40–5.30 (m, 2H, –C*H*=C*H*), 4.51 (s, 2H, –OCH_2), 3.69 (s, 6H, –CH_2–OH), 2.58 (t, J = 7.8 Hz, 2H, –CH_2–Ar), 2.02–1.90 (m, 2H, –CH_2), 1.81–1.57 (m, 6H, –CH_2), 1.40–1.27 (m, 14H, –CH_2), 0.88 (t, J = 6.5 Hz, 3H, –CH_3); ^{13}C NMR (75 MHz, $CDCl_3$) δ = 167.8, 154.7, 142.8, 127.7, 127.5, 127.1, 120.2, 112.8, 109.5, 64.9, 59.8, 58.8, 33.7, 30.3, 29.6, 29.5, 29.5, 29.1, 27.4, 27.4,27.2, 27.1, 27.1, 26.7, 24.9, 20.4, 11.8.

General procedure for the synthesis of *N*-acyl dopamines 8a,b. To the stirred solution of methyl 2-(3-alkyl phenoxy) acetates **3a,b** (1.0 mmol) in dichloromethane (3 mL) and triethylamine (1.2 mmol), added the solution of O-benzyl protected dopamine (1.0 mmol) dissolved in dichloromethane in drops under a nitrogen atmosphere with constant stirring for about 12 h. The progress of the reaction was monitored using TLC. After the completion of the reaction, as identified by TLC, the product is extracted with dichloromethane and solvent is evaporated using rotary evaporator. This crude product thus obtained is dissolved methanol and added 10% Pd/C. The reaction mixture was degassed 3 times and the mixture was stirred vigorously under a hydrogen atmosphere for 24 h. The reaction progress was monitored using TLC. After identifying the completion of the reaction, Pd/C was removed by filtration through a Celite bed and the filtrate was concentrated under reduced pressure using a rotary evaporator to obtain the product **8a,b**.

*Compound **8a**.* Isolated as a pale brown solid; mp: 65–67 °C; yield: 78%;^{1}H NMR (300 MHz, $CDCl_3$) δ = 7.20 (t, J = 7.8 Hz, 1H, Ar–H), 6.85 (d, J = 7.8 Hz, 1H, Ar–H), 6.78 (d, J = 8.1 HZ, 1H, Ar–H), 6.72–6.64 (m, 3H, 1H, Ar–H), 6.54 (d, J = 8.1 HZ, 1H, Ar–H), 4.46 (s, 2H, –OCH_2), 3.54 (q, J = 6.6 Hz, 2H, –CH_2–NH), 2.71 (t, J = 6.9 Hz, 2H, –NHCH_2CH_2–Ar), 2.57 (t, J = 7.8 Hz, 2H, –CH_2), 1.59–1.50 (m, 2H, –CH_2), 1.25–1.11 (m, 24H, –CH_2), 0.88 (t, J = 6.6 Hz, 3H, –CH_3); ^{13}C NMR (75 MHz, $CDCl_3$) δ = 169.2, 157.0, 145.1, 144.1, 143.0, 130.4, 129.5, 122.3, 120.7, 115.5, 115.3, 114.8, 111.6, 67.0, 40.5, 35.9, 34.9, 31.9, 31.3, 29.7, 29.6, 29.6, 29.5, 29.3, 22.7, 14.1. $C_{31}H_{47}NO_4$ $[M + H]^+$ = 498.3583; found 498.3622.

*Compound **8b**.* Isolated as brown viscous liquid; yield: 75%; ^{1}H NMR (300 MHz, $CDCl_3$) δ = 7.16–7.10 (m, 1H, Ar–H), 6.80–6.58 (m, 5H, Ar–H), 6.48 (d, J = 8.4 Hz, 1H, Ar–H), 4.39 (s, 2H, –OCH_2), 3.51–3.44 (m, 2H, –CH_2–NH), 2.67–2.61 (m, 2H, –NHCH_2CH_2–Ar), 2.50 (t, J = 7.2 Hz, 2H, –CH_2), 1.55–1.48 (m, 4H, –CH_2), 1.22–1.13 (m, 18H, –CH_2), 0.88–0.75 (m, 3H, –CH_3); ^{13}C NMR (75 MHz, $CDCl_3$) δ = 169.4, 157.0, 145.1, 144.3, 143.1, 139.9, 130.4, 129.5, 122.4, 120.6, 115.6, 114.9, 111.6, 111.5, 67.0, 40.6, 35.9, 34.8, 31.9, 31.7, 31.4, 29.7, 29.6, 29.6, 29.5, 29.4, 29.3, 22.7, 22.6, 22.6, 21.4, 14.1; $C_{31}H_{45}NO_4$ $[M + H]^+$ = 496.3427; found 496.6.

Preparation of gel. In order to achieve a homogeneous solution, a calculated quantity of the gelator taken in a glass vial is heated with an appropriate amount of solvent/oil. Upon cooling the homogeneous solution to room temperature, gelator tends to self-assemble to form a supramolecular architecture, wherein the solvent molecules were trapped by capillary action. In case of hybrid hydrogel, gelator taken in a glass vial is dissolved in DMSO–water (1 : 3 ratio) by the action of heating, which on subsequent cooling to room temperature furnish the gel. The formation of the gel is confirmed by "stable to inversion" method. The heating and cooling were repeated to check the thermo-reversibility and stability of these gels.[35–42]

Morphological study. The morphology of the oleogel and the hydrogel were investigated using optical microscopy and scanning electron microscopy. The gel was prepared at critical gelation concentration and placed over a glass plate and viewed using Carl Zeiss Axio Scope A1 fluorescent/phase-contrast microscope. Xerogel was used for SEM analysis.

X-ray diffraction and molecular modeling. For SAXRD analysis, a small portion of xerogel prepared from compound **6a** and **7a** and diffraction pattern was obtained on a BRUKER-binary V3 diffractometer system. ChemDraw Professional 16 and Mercury – The Cambridge Crystallographic Data Centre (CCDC) software was used to obtained MM2 energy minimized diagram and 3-D structure visualization respectively. The possible hydrogen bond formation is represented by a red dotted line.

Rheological measurements. The visco-elastic behaviour of the hydrogel obtained from 6a and 7a and the respective composite hydrogel was identified using a stress-controlled rheometer (Anton Paar 302 rheometer) equipped with steel-coated parallel plate geometry of 25 mm diameter. The rheological behaviour of the gels was investigated by keeping the gel sample over the parallel plate at 23 °C. 1 mm gap has been maintained between two parallel plates and the excess gel squeezing out of the parallel plate was trimmed and the measurements were done.

Conflicts of interest

There are no conflicts to declare.

Acknowledgements

Financial support from the Science and Engineering Research Board, Department of Science and Technology, India (sanction order no: CRG/2018/001386) and SPARC, Ministry of Human Resource Development, India (SPARC/2018–2019/P263/SL) is gratefully acknowledged. The authors thank SASTRA Deemed University and National Institute of Technology Warangal for the infrastructure facilities. SN thank INYAS, INSA, Govt of India for membership.

References

1 X. Du, J. Zhou, J. Shi and B. Xu, *Chem. Rev.*, 2015, **115**, 13165–13307.
2 J. Zhou, J. Li, X. Du and B. Xu, *Biomaterials*, 2017, **129**, 1–27.
3 J. Y. C. Lim, Q. Lin, K. Xue and X. J. Loh, *Mater. Today Adv.*, 2019, **3**, 100021.
4 E. R. Triboni, T. B. F. Moraes and M. J. Politi, in *Nano Design for Smart Gels*, Elsevier, 2019, pp. 35–69.
5 S. Panja, A. Panja and K. Ghosh, *Mater. Chem. Front.*, 2021, **5**, 584–602.
6 M. C. Muñoz, G. Blay, I. Fernández, J. R. Pedro, R. Carrasco, M. Castellano, R. Ruiz-Garcia and J. Cano, *CrystEngComm*, 2010, **12**, 2473–2484.
7 D. Ghosh, M. T. Mulvee and K. K. Damodaran, *Molecules*, 2019, **24**, 3472.
8 M. Frauenkron, J.-P. Melder, G. Ruider, R. Rossbacher and H. Höke, Ethanolamines and Propanolamines, in *Ullmann's Encyclopedia of Industrial Chemistry*, 2001, vol. 31, pp. 405–431, DOI: 10.1002/14356007.a10_001.
9 L. Frkanec and M. Žinić, *Chem. Commun.*, 2010, **46**, 522–537.
10 M. Çolak, D. Bariş, N. Pirinççioğlu and H. Hoşgören, *Turk. J. Chem.*, 2017, **41**, 658–671.
11 M. Jokić, V. Čaplar, T. Portada, J. Makarević, N. Š. Vujičić and M. Žinić, *Tetrahedron Lett.*, 2009, **50**, 509–513.
12 M. Löfman, J. Koivukorpi, V. Noponen, H. Salo and E. Sievänen, *J. Colloid Interface Sci.*, 2011, **360**, 633–644.
13 A. Valkonen, M. Lahtinen, E. Virtanen, S. Kaikkonen and E. Kolechmainen, *Biosens. Bioelectron.*, 2004, **20**, 1233–1241.
14 M. Zaboli, H. Raissi, N. R. Moghaddam and F. Farzad, *J. Mol. Liq.*, 2020, **301**, 112458.
15 S. Zhang, J. Hou, Q. Yuan, P. Xin, H. Cheng, Z. Gu and J. Wu, *Chem. Eng. J.*, 2020, **392**, 123775.
16 S. Loganathan, Y. Guo, W. Jiang, T. Radovits, M. Ruppert, A. A. Sayour, M. Brune, P. Brlecic, P. Gude, A.-I. Georgevici, B. Yard, M. Karck, S. Korkmaz-Icöz and G. Szabó, *Pharmacol. Res.*, 2019, **150**, 104503.
17 N. Alipour and H. Namazi, *Mater. Sci. Eng. C*, 2020, **108**, 110459.
18 S. Lee, S. Kim, J. Park and J. Y. Lee, *Int. J. Biol. Macromol.*, 2020, **151**, 1314–1321.
19 G. Zeng, K. Wei, D. Yang, J. Yan, K. Zhou, T. Patra, A. Sengupta and Y.-H. Chiao, *Colloids Surf., A*, 2020, **586**, 124142.
20 J. Ding, H. Wu and P. Wu, *J. Membr. Sci.*, 2020, **598**, 117658.
21 Y. Lv, H.-C. Yang, H.-Q. Liang, L.-S. Wan and Z.-K. Xu, *J. Membr. Sci.*, 2015, **476**, 50–58.
22 H. Li, H. Lin, X. Wang, W. Lv and F. Li, *ACS Appl. Mater. Interfaces*, 2019, **11**, 36469–36475.
23 S. Zhao, Z. Bai, B. Wang, T. Tian and Z. Hu, *Sep. Purif. Technol.*, 2020, **241**, 116633.
24 Z. Yan, Y. Zhang, H. Yang, G. Fan, A. Ding, H. Liang, G. Li, N. Ren and B. Van der Bruggen, *Chem. Eng. Res. Des.*, 2020, **157**, 195–214.
25 Y. Liu, K. Ai and L. Lu, *Chem. Rev.*, 2014, **114**, 5057–5115.
26 V. S. Balachandran, S. R. Jadhav, P. K. Vemula and G. John, *Chem. Soc. Rev.*, 2013, **42**, 427–438.
27 J. R. Silverman, M. Samateh and G. John, *Eur. J. Lipid Sci. Technol.*, 2016, **118**, 47–55.
28 P. Anilkumar, *Cashew nut shell liquid: A goldfield for functional materials*, 2017.
29 T. G. Barclay, K. Constantopoulos and J. Matisons, *Chem. Rev.*, 2014, **114**, 10217–10291.
30 M. S. Behalo, E. Bloise, L. Carbone, R. Del Sole, D. Lomonaco, S. E. Mazzetto, G. Mele and L. Mergola, *J. Exp. Nanosci.*, 2016, **11**, 1274–1284.
31 L. Faure, S. Nagarajan, H. Hwang, C. L. Montgomery, B. R. Khan, G. John, P. Koulen, E. B. Blancaflor and K. D. Chapman, *J. Biol. Chem.*, 2014, **289**, 9340–9351.
32 Y. S. Prasad, S. Miryala, K. Lalitha, K. Ranjitha, S. Barbhaiwala, V. Sridharan, C. U. Maheswari, C. S. Srinandan and S. Nagarajan, *ACS Appl. Mater. Interfaces*, 2017, **9**, 40047–40058.
33 K. Lalitha, V. Sridharan, C. U. Maheswari, P. K. Vemula and S. Nagarajan, *Chem. Commun.*, 2017, **53**, 1538–1541.
34 G. P. Sarvepalli, D. K. Subbiah, K. Lalitha, S. Nagarajan and J. B. B. Rayappan, *J. Mater. Sci.: Mater. Electron.*, 2020, **31**, 1594–1603.
35 K. Lalitha, Y. S. Prasad, C. U. Maheswari, V. Sridharan, G. John and S. Nagarajan, *J. Mater. Chem. B*, 2015, **3**, 5560–5568.
36 K. Lalitha and S. Nagarajan, *J. Mater. Chem. B*, 2015, **3**, 5690–5701.
37 K. Lalitha, Y. S. Prasad, V. Sridharan, C. U. Maheswari, G. John and S. Nagarajan, *RSC Adv.*, 2015, **5**, 77589–77594.
38 K. Lalitha, K. Gayathri, Y. Prasad, R. Saritha, A. Thamizhanban, C. Maheswari, V. Sridharan and S. Nagarajan, *Gels*, 2017, **4**, 1.
39 Y. S. Prasad, B. Saritha, A. Tamizhanban, K. Lalitha, S. Kabilan, C. U. Maheswari, V. Sridharan and S. Nagarajan, *RSC Adv.*, 2018, **8**, 37136–37145.
40 A. Thamizhanban, S. Balaji, K. Lalitha, Y. Prasad, R. Vara Prasad, R. Arun Kumar, C. U. Maheswari, V. Sridharan and S. Nagarajan, *J. Agric. Food Chem.*, 2020, **68**, 14896–14906.
41 O. A. Zhikol, S. V. Shishkina, V. V. Lipson, A. N. Semenenko, A. V. Mazepa, A. V. Borisov and P. V. Mateychenko, *New J. Chem.*, 2019, **43**, 13112–13121.
42 E. R. Draper and D. J. Adams, *Langmuir*, 2019, **35**, 6506–6521.
43 J. Wang and X. Yan, *Nano/Micro-Structured Materials for Energy and Bio-medical Applications* 2018, pp. 205–226.
44 B. Hu, W. Sun, B. Yang, H. Li, L. Zhouu and S. Li, *AAPS PharmSciTech*, 2018, **19**, 2288–2300.

45 V. R. Aldilla, R. Chen, A. D. Martin, C. E. Marjo, A. M. Rich, D. S. Black, P. Thordarson and N. Kumar, *Sci. Rep.*, 2020, **10**, 770.
46 A. Pasc, F. O. Akong, S. Cosgun and C. Gérardin, *Beilstein J. Org. Chem.*, 2010, **6**, 973–977.
47 B. Adhikari, G. Palui and A. Banerjee, *Soft Matter*, 2009, **5**, 3452–3460.
48 C. A. Baladasare and P. G. Seybold, *J. Phys. Chem. A*, 2021, **125**, 3600–3605.
49 N. Goyal, H. P. R. Mangunuru, B. Parikh, S. Shrestha and G. Wang, *Beilstein J. Org. Chem.*, 2014, **10**, 3111–3121.
50 E. R. Draper and D. J. Adams, *Chem. Soc. Rev.*, 2018, **47**, 3395–3405.
51 V. M. P. Vieira, L. L. Hay and D. K. Smith, *Chem. Sci.*, 2017, **8**, 6981–6990.
52 H. Huang, X. Qi, Y. Chen and Z. Wu, *Saudhi Pharm. J.*, 2019, **27**, 990–999.